European Journal of Pharmaceutical Sciences 191 (2023) 106609

Contents lists available at ScienceDirect

European Journal of Pharmaceutical Sciences

journal homepage: www.elsevier.com/locate/ejps

A dry powder formulation for peripheral lung delivery and absorption of an anti-SARS-CoV-2 ACE2 decoy polypeptide

Stefania Glieca [a], Davide Cavazzini [b], Elisabetta Levati [b], Valentina Garrapa [c], Angelo Bolchi [b], Valentina Franceschi [d], Simone Odau [e], Simone Ottonello [b], Gaetano Donofrio [d], Jonas Füner [e], Fabio Sonvico [a,f], Ruggero Bettini [a,f], Barbara Montanini [b,*], Francesca Buttini [a,f,*]

[a] Food and Drug Department, University of Parma, Parco Area delle Scienze 27/A, Parma 43124, Italy
[b] Department of Chemistry, Life Sciences and Environmental Sustainability, University of Parma, Parco Area delle Scienze 27/A, Parma 43124, Italy
[c] Preclinics Italia srl, via Nazario Sauro 3, Parma 43121, Italy
[d] Department of Medical Veterinary Science, University of Parma, via del Taglio 10, Parma 43126, Italy
[e] Preclinics GmbH, Wetzlarer Str. 20, Potsdam 14482, Germany
[f] Interdepartmental Center for Innovation in Health Products, Biopharmanet_TEC, University of Parma, Parco Area delle Scienze 27/A, Parma 43124, Italy

ARTICLE INFO

Keywords:
Dry powder inhaler
Biologics to the lungs
Particle engineering
Trehalose
SARS-CoV-2

ABSTRACT

One of the strategies proposed for the neutralization of SARS-CoV-2 has been to synthetize small proteins able to act as a decoy towards the virus spike protein, preventing it from entering the host cells. In this work, the incorporation of one of these proteins, LCB1, within a spray-dried formulation for inhalation was investigated. A design of experiments approach was applied to investigate the optimal condition for the manufacturing of an inhalable powder. The lead formulation, containing 6% w/w of LCB1 as well as trehalose and L-leucine as excipients, preserved the physical stability of the protein and its ability to neutralize the virus. In addition, the powder had a fine particle fraction of 58.6% and a very high extra-fine particle fraction (31.3%) which could allow a peripheral deposition in the lung. The *in vivo* administration of the LCB1 inhalation powder showed no significant difference in the pharmacokinetic from the liquid formulation, indicating the rapid dissolution of the microparticles and the protein capability to translocate into the plasma. Moreover, LCB1 in plasma samples still maintained the ability to neutralize the virus. In conclusion, the optimized spray drying conditions allowed to obtain an inhalation powder able to preserve the protein biological activity, rendering it suitable for a systemic prevention of the viral infection via pulmonary administration.

1. Introduction

In the last few decades, biologics have become the most clinically relevant therapeutic options for several diseases. Most of the biologics approved and already on the market are liquids or lyophilized powders for injection. This type of formulation often needs to be administered by healthcare professionals, giving rise to poor patient acceptability, especially if the treatment is for chronic conditions, and requires cold-chain distribution, storage, and handling (Fathe et al., 2016). The inhalation route can represent an attractive alternative for the delivery of the biologics to achieve either local or systemic effects (Pinto et al., 2021).

Pulmonary administration of proteins can be carried out via a nebulizer or by a dry powder inhaler (DPI). Conversely, pressurized metered dose inhalers are not particularly suitable for the administration of biologics because of the physical instability of protein suspensions in HFA propellants and the very low doses achievable (Fathe et al., 2016). In the case of delivery by nebulization, the protein-containing product is usually formulated as an aqueous solution or suspension and this poses serious nebulization-related stability issues (Bianchera et al., 2023; Brun et al., 2023). A possible alternative, particularly for unstable biologics, relies on the production of a solid formulation (usually by freeze-drying) that is solubilized immediately prior to administration. Further drawbacks of nebulizer-based delivery, in addition to a careful control of biologic integrity both in the formulation and during the nebulization, are the long preparation and administration times, the need for thorough cleaning of the device prior to re-use and a source of electric power. Most of the above limitations would be

* Corresponding authors.
E-mail addresses: barbara.montanini@unipr.it (B. Montanini), francesca.buttini@unipr.it (F. Buttini).

https://doi.org/10.1016/j.ejps.2023.106609
Received 7 June 2023; Received in revised form 22 September 2023; Accepted 12 October 2023
Available online 13 October 2023

overcome by conversion of the biologic into a respirable solid form and its administration by a DPI. It is known that biomolecules tend to be more stable as solid rather than liquid forms at room temperature and an inhalable dry powder, can be obtained by a controlled drying process conducted in the presence of selected excipients that guarantee the stability and long-term shelf-life of the biologic (Chen et al., 2021).

Recently, with the spread of the severe acute respiratory syndrome coronavirus 2 (SARS-CoV-2), the need to re-evaluate the potential of the delivery of biological drugs or vaccines to the lung emerged. Key features of SARS-CoV-2 compared to previous coronaviruses, such as SARS-CoV and MERS-CoV, are its extremely high human-to-human transmission rate and ability to attack multiple organs in addition to the lungs (Li et al., 2020). Such multisite infection capability is explained by the occurrence of the angiotensin-converting-enzyme-2 (ACE2), the SARS-CoV-2 interaction receptor, in a variety of extra-pulmonary tissues such as heart, gastrointestinal system, kidney, liver, and the central nervous system (CNS) (Su et al., 2016). The outer surface of SARS-CoV-2 is covered by a spike glycoprotein (Majumder and Minko, 2021) whose Receptor Binding Domain (RBD) initiates host cell penetration through direct interaction with the ACE2 receptor. The latter is present in the airways epithelia and at particularly high levels on alveolar epithelial type II cells which the virus causes to collapse leading to pneumonia and acute respiratory distress syndrome (ARDS) in the most severe cases (Alipoor et al., 2020).

Among the various treatments proposed for the management of SARS-CoV-2 infection, an alternative way of preventing virus internalization may rely on a so-called "decoy approach". In detail, a macromolecular mimic of the ACE2 receptor ectodomain acts as high-affinity viral trap capable of interfering with virus entry mediated by interaction of the RBD with the endogenous ACE2 receptor. However, the neutralization capacity of a specific decoy may differ depending upon the subset of virus variants (Huang et al., 2022).

Multiple ACE2 mimetic, highly thermostable small proteins binding the spike RBD with picomolar affinity have been generated through a structural design approach (Cao et al., 2020; Case et al., 2021). The lead binder, designated as LCB1, a *de novo* designed three-helix protein, has been shown to be protective against lung disease caused by a subset of SARS-CoV-2 variants in human ACE2-expressing transgenic mice when administered by the intranasal route at a dosage of 2.5 mg/kg (Case et al., 2021). An even lower dosage was found to be effective when administered prior to SARS-CoV-2 exposure (Case et al., 2021).

The aim of this work was to investigate and design a dry powder delivery system for small proteins to the lungs. The LCB1 decoy was used as a model protein to be converted into a highly stable and respirable powder by spray drying. The effect of different excipients and process parameters on yield, stability and aerodynamic properties of the resulting powders were investigated systematically. The pharmacokinetics and the maintenance of the LCB1 biological activity after the administration of the powder in rats was assessed.

2. Materials and methods

2.1. Materials

Trehalose (batch no. 07/4801) and L-leucine (batch no. Q0096002) were purchased from A.C.E.F. Spa (Italy) and mannitol Pearlitol 50C (batch no. e 869 K) from Roquette (France). Lactose (Respitose SV003, batch no. 10258398) was purchased from DMV International (Netherlands), and glycine (batch #SLCC7952) from Sigma-Aldrich (USA). Ultrapure water (0.055 μS/cm) was produced by reverse osmosis (PureLab Pulse, Elga-Veolia, Italy).

2.2. Expression and purification of LCB1 protein

A codon-optimized sequence coding for an N-terminal 6xHis- and c-myc tagged version of the LCB1 protein was chemically synthesized (GenScript Biotech Corp., USA) and inserted into the NcoI-XhoI restriction sites of the pET28 plasmid (Novagen, Sigma Aldrich, USA). The resulting construct was transformed into *Escherichia coli* BL21 codon plus (DE3) cells and expression of the recombinant LCB1 protein was carried out for 24 h at 20 °C under auto-induction conditions (Auto Induction Medium, AIM - LB broth base; Formedium, UK). LCB1 was comprised of 87 amino acid residues (detailed sequence in the supplementary materials), with a predicted molecular mass of 10.35 kDa and a pI of 4.93. After sonication in lysis buffer (25 mM Tris-HCl, pH 8.0, 0.3 M NaCl) supplemented with Protease Inhibitor Cocktail (Sigma-Aldrich, USA), the lysate was centrifuged for 10 min at 9,000 g and the resulting supernatant was subjected to metal-affinity chromatography (ÄKTA Pure 25M chromatographic system, GE Healthcare, USA; flow rate: 2.5 ml/min) on a HisTrap FF 5 ml column (Cytiva, USA) pre-equilibrated in 25 mM Tris-HCl (pH 7.8), 20 mM imidazole, 0.3 M NaCl (buffer A). After extensive washing, protein was eluted by applying an 18 min linear gradient to buffer B (same as buffer A but containing 500 mM imidazole). LCB1 containing fractions, identified by SDS-polyacrylamide gel electrophoresis (SDS-PAGE; 15% polyacrilamide), were pooled and the buffer was changed to phosphate buffer saline (PBS) by fractionation on a HiTrap column (Cytiva; 1.5 ml/min) pre-equilibrated in PBS.

2.3. Characterization of LCB1 protein

The purified LCB1 product (final yield of ~20 mg/L of bacterial culture) was checked again by SDS-PAGE, quantified by UV-Vis spectrophotometry (using a calculated extinction coefficient of 9970 M^{-1} cm^{-1}) by measuring its absorbance at 280 nm, and stored at -80 °C. The native molecular weight of the LCB1 protein was estimated by size exclusion chromatography (SEC) analysis performed on a 3 mL Superose 6 Increase 5/150 GL column (GE Healthcare, US, flow rate: 0.25 mL/min) or a 3 mL Superdex 200 Increase 5/150 GL column (GE Healthcare, flow rate: 0.3 mL/min) equilibrated in 25 mM Tris-HCl buffer (pH 7.5), 150 mM NaCl.

Far-UV circular dichroism (CD) spectroscopic analysis (190–260 nm; average of 4 scans) was performed on each LCB1 sample (diluted to 5 μM in 10 mM phosphate buffer, pH 7.5) at 25 °C with a Jasco J-1500 Spectropolarimeter (0.1 cm path-length cuvette, bandwidth of 1 nm, data pitch of 0.5 nm, response time of 4 s).

2.4. Pre-formulation and design experiments to develop a manufacturing process for spray-dried powders

The pharmaceutical development of the powders was carried out in three phases, the first two using blank powders *(i.e.,* without the LCB1 protein) and the last one including the protein. The three steps were aimed at: (i) identifying the most suitable bulking agent, (ii) optimizing the overall composition and (iii) producing an optimized LCB1-containing powder formulation.

The first set of powders was produced using mannitol, lactose or trehalose plus glycine or L-leucine using different buffers to dissolve the various components. PBS at pH 7.4 or phosphate buffer (PB) at pH 7.25 (NaCl and KCl-free) were employed. The components of these placebo powders are reported in Table 1.

Powders were produced employing a B-290 mini-spray dryer (Büchi Laboratoriums-Technik, Switzerland) using air as the drying gas, keeping a set of specific spray drying parameters constant: 125 °C inlet temperature, aspiration at 720 L/h, 3 mL/min feed rate, nozzle 0.7 mm and a feed solution concentration of 0.2% (w/v). The yield of the spray drying process was calculated as the percentage ratio (%) of the weight of the powder recovered from the spray dryer collector to the weight of the dry materials in the feed solution.

For the second set of formulations, a full factorial design of experiment (DoE) was applied with three factors at two levels with one central point ($2^3 + 1$), to study the effect of the combinations of the selected process parameters and composition factors on the critical quality

Table 1
Composition of the placebo powders (*i.e.* powders without LCB1) prepared and tested in the pre-formulation experiments.

Powder #	Trehalose (%w/w)	Lactose (%w/w)	Glycine (%w/w)	L-leucine (% w/w)	Buffer Type * and Salt Conc. (mg/ml)
A	85	-	15	-	PBS (4.8)
B	85	-	15	-	$PBS_{1/2NaCl}$ (3.2)
C	85	-	15	-	PB (2.7)
D	90	-	10	-	PBS (4.8)
E	95	-	-	5	PB (2.7)
F	-	85	15	-	PBS (4.8)
G	-	85	15	-	PB (2.7)
H	-	90	10	-	PBS (4.8)

* PBS= 50 mM NaCl, 2.5 mM KCl, 10 mM Na_2HPO_4 and 2 mM KH_2PO_4. $PBS_{1/2NaCl}$= 25 mM NaCl, 2.5 mM KCl, 10 mM Na_2HPO_4 and 2 mM KH_2PO_4. PB =14 mM Na_2HPO_4, 6 mM KH_2PO_4.

attributes (CQAs). The DoE matrix was generated using Design Expert software (version 13, Stat-Ease Inc., USA). The process yield (%), the emitted dose (%) and the respirable fraction (%) were used as CQAs. Table 2 illustrates the DoE matrix and the three process parameters investigated: L-leucine concentration (% w/w), feed solution concentration (% w/v) and inlet temperature (°C).

The excipients were dissolved in a PB solution at a concentration of 2.7 mg/mL, corresponding to 8% w/w in the formulation, and spray-dried using the process parameters indicated above; only the inlet temperature was changed in accordance with the DoE.

In the third phase of development, considering the results of the DoE and powder #2 as the lead formulation, a decoy powder (LCB1-DPI) containing 6% (w/w) of LCB1, 8% (w/w) PB salts, 14% (w/w) L-leucine, and 72% (w/w) of trehalose was produced setting 125 °C as inlet temperature and 0.2% (w/v) as the solids concentration of the suspension to be spray dried. Three batches with this composition were produced. For all the batches, the LCB1 concentration in the starting solution was 2 mg/mL.

2.5. *In vitro aerodynamic assessment*

For all blank powders produced in the first two stages of the spray-drying development, the *in vitro* respirability was assessed with a Fast Screening Impactor (FSI, Copley Scientific Ltd., UK). In detail, for each analysis, one hydroxypropyl methylcellulose (HPMC) capsule size 3 (Quali-V-I, Qualicaps Europe, Spain) was filled with 40 mg of powder occupying about the 50% of the capsule volume. The powder was aerosolized in the FSI using a RS01 device (Plastiape, Italy) at 65 L/min to obtain a 4 kPa pressure drop. The FSI was coupled with a SCP5 vacuum pump (Copley Scientific Limited, UK) and a Critical Flow Controller (TPK Copley, Copley Scientific Limited, UK) to set the required flow rate.

Table 2
Matrix of the full-factorial design of experiments. The concentration of PB salts is the 8 % w/w and the weight fraction to reach 100 % w/w of each formulation is represented by trehalose.

Powder #	Factor A L-leucine (% w/w)	Factor B Feed Concentration (% w/v)	Factor C Inlet Temperature (°C)
1	9	0.5	130
2	14	0.2	125
3	4	0.2	125
4	4	0.8	125
5	14	0.8	125
6	14	0.8	135
7	14	0.2	135
8	4	0.8	135
9	4	0.2	135

The device was activated for 3.7 seconds to allow the passage of 4 L of air.

The amount of the powder emitted (ED) by the device after the aerosolization was determined gravimetrically by weighing the device before and after the aerosolization using a Mettler Toledo AX205 balance with a sensitivity of 0.00001 g. The emitted fraction (EF) was calculated as the ratio (%) of the emitted dose to the powder mass loaded in the capsule. Similarly, the fine powder mass with size < 5 μm deposited on the glass microfiber filter (76 mm, Type A/E, Whatman, UK) was measured gravimetrically. The respirable fraction (RF) was expressed as the ratio (%) of the powder recovered on the filter to the emitted dose. Three FSI runs were carried out for each powder.

The LCB1-DPI was additionally characterized in terms of the aerodynamic profile using a Next Generation Impactor (NGI, Copley Scientific Limited, UK). Capsules were filled with 40 mg of powder, containing approximately 2 mg of protein. For the three analyses, the content of an individual capsule was discharged with the RS01 device using the air-flow rate specified above. The powder deposited in the NGI and the amount remained in the device was collected in a 20 mM PB solution (pH 7.25) and the protein content of the powder was determined by UV-Vis spectrophotometry, as described previously.

Quantification of the LCB1 deposited within the impactor allowed the calculation of the aerodynamic parameters. The recovered dose is the mass of the protein recovered in the device and in all the impactor portions: induction port (IP), stages 1 to 7 and Micro Orifice Collector (MOC). The Emitted Dose (ED) is the amount of protein leaving the device and entering the impactor. A cumulative distribution curve was obtained by plotting (GraphPad Prism v. 9.5.1, US) the cumulative percentage of mass less than the stated size cut-off for each NGI stage on a probability scale versus the cut-off diameter of the respective stage on a logarithmic scale. The mass median aerodynamic diameter (MMAD) of the powder is the particle size corresponding to midpoint (50%) of the cumulative distribution curve. The log-probability plot equation allowed the fine particle mass (FPM) to be calculated, representing the mass of particles with an aerodynamic diameter < 5 μm and the extra-fine particle mass (EFPM) < 2 μm. The fine particle fraction (FPF) and the extra-fine particle fraction (EFPF) were expressed as the ratio (%) between the FPM and EPFM and the ED, respectively.

2.6. *Scanning electron microscopy and residual water content*

The morphology of the blank spray-dried lead powder #2, composed of trehalose and L-leucine (78:14) and of the LCB1-DPI was studied by Scanning Electron Microscopy (SEM, Supra 4000, Carl Zeiss, Germany), with an electron high tension (EHT) at 1.00 kV. Samples were dispersed on double-sided adhesive tape pre-mounted on an aluminum stub and analyzed after 30 min of depressurization.

The residual water content in the LCB1-DPI was measured employing a thermogravimetric analyzer (TGA, METTLER Toledo, USA) under a flux of dried nitrogen from 25 °C to 160 °C at a rate of 10 °C/min by integrating the weight loss between 25 and 130 °C.

2.7. *ELISA assays*

Enzyme-linked immunosorbent assay (ELISA) was used to compare the RBD binding capacity of native and spray-dried LCB1. To this end, 100 μl of LCB1 (diluted to a final 2 μM concentration with PBS) were added to the wells of microtitre plates (SpectraPlate-96 HB; Perkin Elmer, Italy). After overnight incubation at 4 °C, the wells were washed three times with 300 μl of PBS containing 0.2% (v/v) Tween-20 (PBS-T) and blocked at 37 °C for 1 h with 400 μl of 3% (w/v) skimmed milk (Sigma-Aldrich, USA) dissolved in PBS. Plates were then washed three times with PBS-T and three-fold serial dilutions (starting from 133 nM) of mouse Fc-tagged receptor binding domain polypeptide (RBD-mFc; GenScript, uSA) were added to the wells and incubated at 37 °C for 1 h. After washing three times with 300 μl of PBS-T, 100 μl of an anti-mouse

IgG (whole molecule) – peroxidase antibody conjugate (A4416, Sigma-Aldrich, USA; diluted 1:1000 in PBS) were added and the plates were incubated at 37 °C for 1 h. After three additional washings with PBS-T, 100 µl of 2,2′-azino-bis (3-ethylbenzthiazoline-6-sulfonic acid) peroxidase substrate (ABTS; SeraCare Life Sciences, USA) were added to each well and following a 30 min incubation at 30 °C, the signal produced by ABTS oxidation was determined by measuring the absorbance at 415 nm with a microplate reader (iMark™ Microplate Absorbance Reader; Bio-Rad, USA).

A reverse ELISA format, with plates pre-coated with 50 µl per well of 2 µM RBD-mFc, was used to quantify LCB1 in the serum or bronchoalveolar lavage fluid (BALF) of LCB1-treated rats. Following overnight incubation at 4 °C, the wells were washed three times with 300 µl of PBS-T and blocked at 37 °C for 1 h with 400 µl of 3% (w/v) skimmed milk (Sigma-Aldrich, USA) dissolved in PBS. Plates were then washed three times with PBS-T and 50 µl of each serum/BALF sample were added to the RBD-mFc pre-coated wells followed by incubation at 37 °C for 1h. After washing three times with 300 µl of PBS-T, 100 µl of horseradish peroxidase-conjugated anti-Myc tag antibody (ab1261, Abcam, USA; diluted 1:10000 in PBS) were added and the plates were incubated at 37 °C for 1 h. Following three additional washings with of PBS-T (300 µl each), 100 µl of ABTS were added to each well and after a 30 min incubation at 30 °C the ABTS oxidation signal was measured at 415 nm as above.

2.8. SARS-CoV-2 pseudovirus neutralization assays

Lentiviral vector-based SARS-CoV-2 S pseudovirus was generated as previously described with minor modifications (Donofrio et al., 2021). Sub confluent HEK 293T cells were co-transfected with pLV-EF1α-(turboGFP-Luc2)-WPRE transfer vector, p8.74 packaging vector, pseudotyping vector coding for three different spike glycoproteins (Wuhan-Hu-1 B.1 Lineage; China; Delta B.1.617.2 Lineage, India; Omicron B.1.1.529 Lineage, Europe) and pREV with PEI (polyethylenimine; Polysciences, Inc., USA) (1 mg/mL in PBS) (ratio 1:2.5 DNA/PEI). Transfected cells were incubated for 48 h at 37 °C with air containing 5% CO_2. Flasks were then frozen (-80 °C) and thawed; transfected cell supernatants containing the S pseudoviruses were clarified by centrifugation, filtered through a 0.45 µm filter (Millipore, Merk, Darmstadt, Germany), aliquoted, titrated by limited dilution and stored at −80 °C. Serum neutralization assays were performed as described previously (Donofrio et al., 2021).

Briefly, S pseudoviruses in 10% FBS were added to microtiter plate wells containing LCB1 in liquid form (solution after purification) or dissolved LCB1-DPI and incubated at room temperature for 1.5 h. A protein-free powder (blank powder) consisting of the spray-dried excipient mixture (trehalose:leucine:salts 78:14:8) was tested as a negative control. Next, 10^4 HEK/ACE2/TMPRRS2/Puro cells were added to each well and incubated for 60 h at 37 °C in a 5% CO_2 atmosphere. Luciferin was then added, just before reading of the microplates with a luminometer (Victor, Perkin Elmer, Italy). The neutralizing activity was expressed as % of pseudovirus entry after treatment in respect to the wells where the pseudovirus was added without treatment. Each treatment was tested in triplicate.

2.9. Pharmacokinetic profiling of the pulmonary delivered LCB1-DPI

Animal studies to evaluate the pharmacokinetics of LCB1 administered intratracheally in liquid form and as spray-dried powder were performed at Preclinics Gmbh (Postdam, Germany) in accordance with German and European animal welfare legislation and under the authorization of the Landesamt für Arbeitsschutz, Verbraucherschutz und Gesundheit (LAVG). Seven Wistar male rats (8-9 weeks-old), allowed to acclimatize for twelve days after transportation, were employed in the pharmacokinetic analysis. A dosage of 0.67 mg LCB1/kg was used for both the liquid and the dry-powder formulation of the protein; the former consisted of the LCB1 purified solution, and the latter was the LCB1-DPI.

Before the intratracheal administration, the animals had been lightly anesthetized with 5% isoflurane and lain back at an angle of 45/50° to avoid backflow of the instilled suspension and to increase penetration into trachea and bronchi. Using a small laryngoscope, a guide wire was inserted into the trachea and used to aid the introduction of a catheter (BD Insyte 22G, Becton, Dickinson & Co., USA) through which the native LCB1 in solution was pipetted into the conus, followed by the injection of 200 µl air to flush the catheter. The dry-powder formulation was administered with a Penn-Century Dry Powder Insufflator ™ (Model DP-4 M, Penn-Century, USA). The powder loaded in the insufflator was delivered into the lungs by the discharge of 4 mL of air. Before the experiment, the amount emitted from the insufflator had been determined by weighing the device before and after delivery. Blood samples (200 µl each) were collected at 1 h, 3 h, 6 h and 24 h post-administration. A broncho-alveolar lavage (BAL) was performed after 48 h and the animals were then exsanguinated by cardiac puncture. Plasma and bronchoalveolar lavage fluid (BALF) samples were stored at -80 °C prior to LCB1 quantification and functional analysis. Finally, diluted sera from LCB1-treated rats were tested in terms of neutralizing activity and expressed as neutralization titer 50 (NT50/ml), *i.e.,* the maximal dilution of antiviral product causing a $\geq$50 % reduction of the luminescent signal. The analysis was performed as described above and each serum sample was tested in triplicate.

2.10. Statistical analysis

Statistical analysis of variance (ANOVA) was performed to determine the significance (p-value) of each factor and their interactions as revealed by the DoE results. A two-way ANOVA test was performed on the ELISA assay and neutralization experiments data reported in the results section below.

3. Results and discussion

3.1. Pre-formulation and experimental design

The preparation a powder suitable for inhalation involves the drying of a solution or suspension containing the biologic drug, together with its excipients. The presence of the active moiety in a solid state helps to prevent protein aggregation or inactivation. Among the possible drying techniques, spray drying represents a means of engineering the size, shape, and density of particles, which should improve their aerosolization performance. It is preferred to freeze-drying which produces dry cakes that usually have poor aerosolization characteristics (Eedara et al., 2021). In addition, spray drying consumes less energy, is more cost-effective, has good batch-to-batch reproducibility and has the capability to be used for large-scale production (Eedara et al., 2021).

In spray drying, the protein, being exposed to an air-liquid interface and subjected to thermal stress, might be destabilized or irreversibly denatured. Carbohydrates are known to act as protein stabilizers due to their ability to replace the hydrogen bonds formed with water by the hydrated form of the protein, which is thus maintained in its native state (Pinto et al., 2021).

Firstly, different ‘placebo’ (*i.e.*, protein-free) powders containing mannitol, lactose or trehalose as prototype excipients, plus different amounts of saline buffer, were produced to investigate their suitability as formulation platforms.

Buffer salts are important to maintain optimal pH and ionic strength for protein conformational integrity and biological activity (Mutukuri et al., 2022) and salt composition can affect the chemical stability of the protein during and after the drying process. On the other hand, salts tend to induce phase separation leading to the formation of cohesive, often poorly dispersible particles (Mutukuri et al., 2022), and their amount and type thus require optimization during the pre-formulation phase.

Standard PBS, the same buffer containing a halved NaCl concentration ($PBS_{1/2\ NaCl}$) or the buffer lacking any salt supplementation (PB) were selected in the preliminary formulation investigation based on their capability to solubilize and stabilize the LCB1 protein. The yield of the spray drying process, plus EF% and RF% as indicators of powders respirability were the parameters used to judge the quality of the product.

Mannitol was ruled out as a bulking agent from the very beginning because of the extremely low yield (2%) produced by spray drying. In fact, most of the powder stuck to the cyclone walls in a form that was impossible to collect. This behavior is likely explained by the tendency of mannitol to crystalize and cause phase separation in the presence of salts, especially NaCl (Costantino et al., 1998). On the other hand, production yields as high as 60% were achieved with lactose or trehalose in the presence of either PBS, $PBS_{1/2\ NaCl}$ or PB.

As shown in Fig. 1 the respirability decreased significantly with the increase in the salt concentration. In fact, by comparing the trehalose: glycine (85:15) formulations, the respirable fraction of 20% obtained when the buffer was PB, decreased significantly both with $PBS_{1/2\ NaCl}$ (p-value = 0.009) and with PBS (p-value < 0.001). In general, regardless of the combination of excipients used, the RF was at the lowest value with the highest salt concentration but increased markedly upon NaCl reduction or elimination, reaching a maximal value of 40% in the case of PB associated with a trehalose: L-leucine 95:5 mixture.

This pre-formulation exploratory phase allowed the identification of trehalose:L-leucine 95:5 mixture along with PB as the best performing combination in terms of aerodynamic behavior. Although the RF of lactose-containing powder was also acceptable (~ 28%), this excipient was not further investigated because lactose, being a reducing sugar, might undergo a Maillard reaction upon interaction with protein amino groups (Fathe et al., 2016).

Formulation optimization was then performed with a DoE aimed at investigating the effect of the amount of L-leucine, feed solution concentration and inlet temperature on the main CQAs of the placebo powders. In the case of all three inlet temperatures used, the outlet temperature value was lower than 85 °C, a value below which the protein had been shown to be stable when investigated by circular dichroism (data not shown, (Cao et al., 2020)). The results of DoE analysis for the nine blank powders (see Table 2 for details on the compositional and spray-drying process parameters of each powder), based on the three selected CQAs, are reported in Table 3.

Despite the yield ranging from 35% to 80%, no significant influence

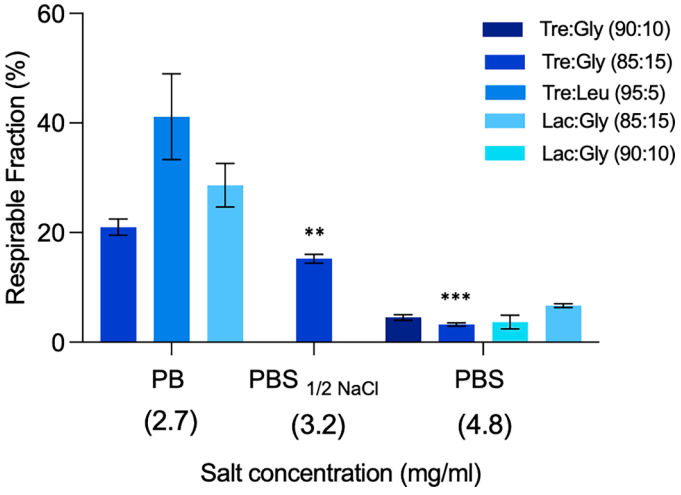

Fig. 1. Respirable fraction of the eight placebo powders obtained in the pre-formulation studies starting from three different buffer types and trehalose or lactose as bulking agent (statistical analysis: RF of Tre:Gly 85:15 of the two PBS versus PB, ** p<0.01; ***p<0.001), (n=3, mean ± std. dev.).

Table 3
Yield and aerodynamic performance of the nine powders prepared with the full factorial design of experiments. EF and RF experiments were conducted in triplicate and results reported as mean value ± SD.

Powder #	Yield (%)	Emitted fraction (%)	Respirable fraction (%)
1	64.5	86.6±2.5	48.5±5.0
2	56.4	93.9±1.2	52.8±6.7
3	35.0	70.7±6.4	40.2±5.8
4	71.8	94.7±2.5	37.0±2.6
5	66.7	97.2±1.9	20.5±0.2
6	55.7	96.4±3.1	24.1±0.3
7	67.4	93.3±2.5	52.8±10.8
8	45.1	82.9±0.9	16.7±1.9
9	80.1	79.7±9.5	47.2±3.9

on production yield by the various factors examined was detectable by ANOVA (p= 0.8632). The two powders with the lowest and the highest yields had been produced at different inlet temperatures: when set at 125 °C, a 35% yield was obtained (powder #3), which increased to 80% at an inlet temperature of 135 °C (powder #9). However, considering all the batches, no relationship was observed between temperature and yields indicating that other factors impacted production efficiency.

The degree of significance and the effect of the factors and their interactions on EF are illustrated by the Pareto chart in Fig. 2A. Statistical analysis indicated that L-leucine concentration had a significant, positive effect on the emitted fraction (*p*-value of 0.0397). The EF for all blank powders was higher than 70% (Table 3) and reached a value of 97% in the case of powder #5 where the level of the lubricant excipient was 14%. The effect on the EF of the other factors investigated was not statistically significant.

The beneficial role of L-leucine on EF can be explained by the fact that, during the drying process, it forms a solid shell around the droplet which deforms to different degrees because of plastic expansion, giving roundish particles with a corrugated surface (Alhajj et al., 2021). The morphology exhibited by powder #2, as confirmed by SEM (Fig. 3A), confers two positive properties to the powder: a greater emission from the inhaler and a higher respirability (Table 3). Similar values were obtained for powder #7 which, although having identical composition, was dried at a higher temperature. The first property mentioned above can be explained by the fact that surface roughness reduces inter-particle interactions mediated by Van der Waals' forces, making the microparticles less cohesive and thus increasing the amount emitted from the device. The second property can be ascribed to the hollow appearance of the microparticles, which reduces their density, leading to an increase in the FPF and a reduction in the MMAD (Alhajj et al., 2021).

Regarding the final CQA investigated (RF, Fig. 2B), the concentration of the feed solution had a statistically significant negative effect on this parameter (*p*-value 0.0044). The RF value varied from 16.7% to 52.8%, when the feed solution was set at 0.8% w/v and 0.2% w/v, for powders #8 and #2, respectively (Table 3).

The above results thus indicate that an increase in the amount of the solute in the solution to be spray-dried leads to an increase of the aerodynamic diameter of the particles. This finding is in line with a previous work (Vehring, 2008), which showed direct correlation between these two factors as shown in Eq. (1),

$$d_{ae} = \sqrt[6]{\frac{\rho P}{\rho}}\sqrt[3]{\frac{cF}{\rho}}\ d_D \qquad (1)$$

where d_{ae} is the aerodynamic diameter, ρP is the particle density, ρ is true density of the material, cF is the concentration of the feed solution and d_D is the diameter of the droplets.

High inlet temperature during the spray drying of a protein can present an issue for its stability. Accordingly, although the composition of powder #7 produced the same aerodynamic behavior as powder #2,

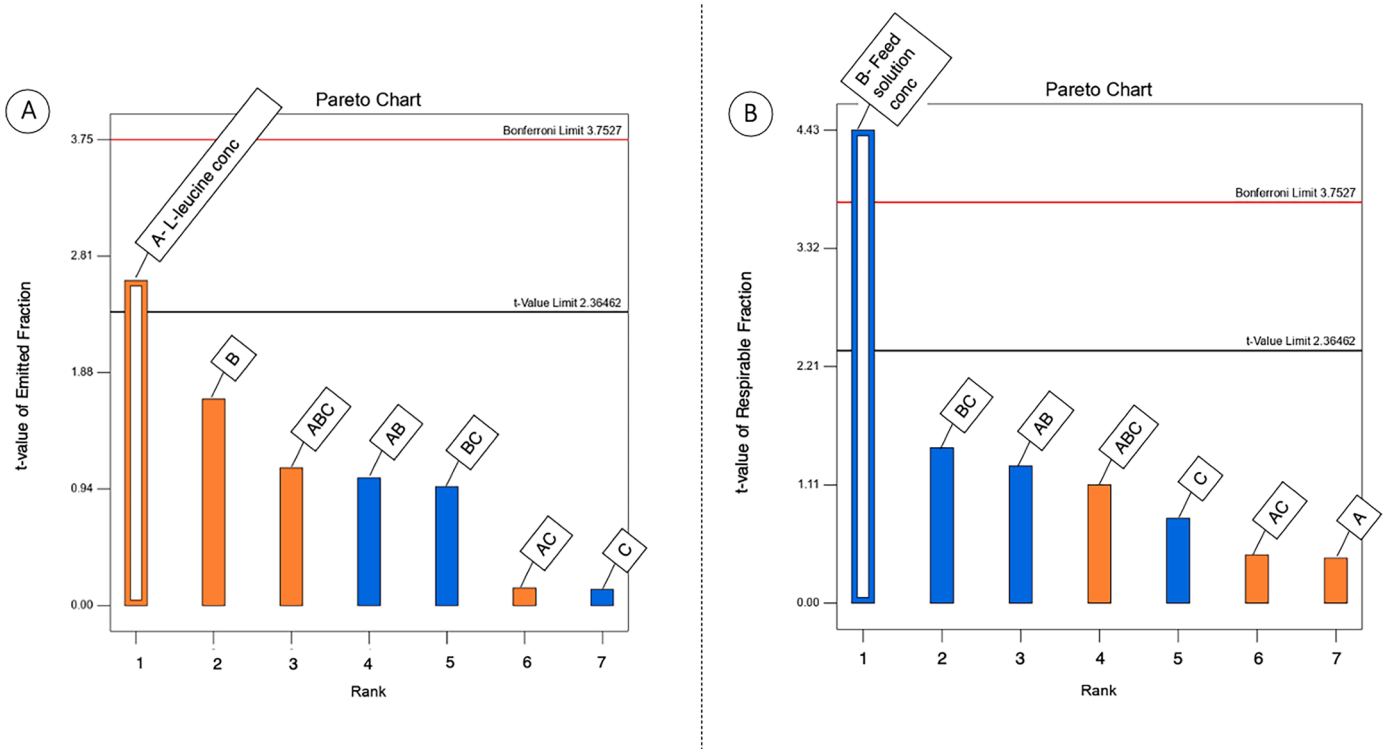

Fig. 2. Pareto chart illustrating the rank of the t-values corresponding to the effect of each factor and their interactions on the emitted fraction (**A**) and on the respirable fraction (**B**). Empty bar: significant; full bars: non-significant; blue bars: negative effects; orange bars: positive effect. List of factors: A: L-leucine concentration; B: feed solution concentration; C: inlet temperature. The orange line corresponds to the Bonferroni limit and the black one to the t-value limit for significance.

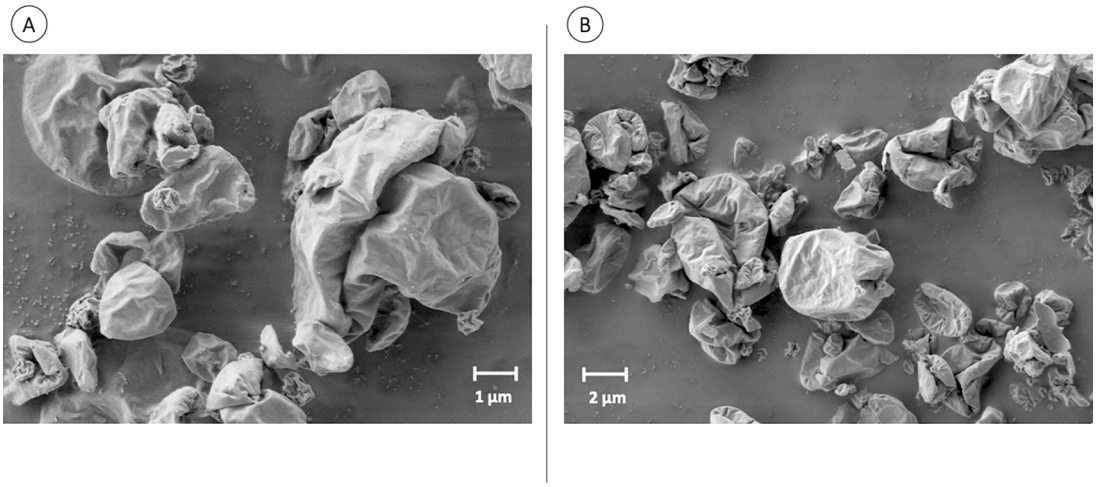

Fig. 3. SEM image of the decoy-free lead powder #2 of the DoE containing trehalose (78%) and leucine (14%) (Mag. 20K x) **(A)** and of the LCB1-DPI (Mag. 10K x) **(B).**

the operational parameters employed for the latter (125 °C) were considered as optimal and adopted for the subsequent formulation of LCB1 protein-containing powders.

3.2. Production and structural integrity of the LCB1 dry powder

In the third phase of development, an LCB1-loaded powder (LCB1-DPI) was produced by applying the optimized formulation resulting from the DoE (powder #2) keeping the amount of L-leucine the same but reducing the amount of sugar to allow formulation space for the protein. The reliability of transferring blank powder data to the production of a protein-containing powder was supported by the results of previous workers (Rossi et al., 2021), showing that the addition of a small-sized protein (HPV16 L2-thioredoxin conjugate of 18 kDa) did not appreciably modify the overall features of the spray-dried powder.

The LCB1-DPI thus consisted of 6% of LCB1 protein, 8% PB salts, 14% L-leucine and 72% trehalose, all concentrations expressed as w/w. In this way, 2.4 mg of protein (theoretical therapeutic dose of LCB1), were incorporated in a total of 40 mg of powder. Such a LCB1 decoy dose, once dissolved in the limited volume of the pulmonary fluid (20-30 mL), would lead to a local concentration (~ 10 µM) which is at least 1000-fold higher than the nanomolar concentrations previously shown

to be effective for SARS-CoV-2 neutralization (Cao et al., 2020).

Spray drying of the LCB1-DPI powder produced a yield of about 65%. Furthermore, in good agreement with the theoretical value, the fractional content of LCB1 was 5.7±0.4%, indicating that the protein primary structure tolerated the heat stress induced by the spray drying process. The process efficiently dried the protein solution since the level of residual free water determined by TGA was of 2.14±0.27%.

The structural integrity of the protein within the LCB1-DPI was assessed by SDS-PAGE, SEC and circular dichroism analyses (Fig. 4). SDS-PAGE fractionation was used to detect potential degradation products and/or molecular mass alterations that might be caused by the spray drying process. As shown in Fig. 4A, no appreciable differences in molecular weight, nor any extra bands resulting from protein degradation could be detected in the powder sample compared to the control represented by the native protein in solution. Similarly, no appreciable differences between the two protein samples were revealed by SEC analysis, as they both eluted as single, symmetrical peaks, with an apparent MW of approximately 23 kDa (Fig. 4B). The lack of any earlier additional peaks corresponding to higher molecular weight in the spray-dried protein chromatogram indicates that the native state of LCB1 is fully preserved upon spray drying, with no detectable aggregates or other types of thermal stress induced higher-order species. The far-UV circular dichroism spectra of LCB1 that were collected before and after spray drying (Fig. 4C) were virtually identical, displaying a profile typical of alpha secondary structures, as expected for this protein in its native form (Cao et al., 2020).

The above results were consistent across the three LCB1 powder batches, thus indicating the robustness of expression-purification of the recombinant protein as well as of its conversion into a dry powder by an optimized spray drying process. This outcome was certainly favored by the high physicochemical stability of single-chain ACE2-mimicking polypeptides, which makes them amenable to various (even relatively harsh) formulation production processes that would be less tolerated by oligomeric multi-chain mAbs.

3.3. Aerodynamic and stability properties of the LCB1-DPI

The *in vitro* respirability of the LCB1-DPI was extensively investigated with a multistage impactor using a powder mass of 40 mg which, according to the batch drug content, corresponded to 2.16 mg of protein. The deposition of the protein in the NGI and the aerodynamic parameters are illustrated in in Fig. 5 and Table 4, respectively.

The LCB1-DPI was efficiently emitted (89.8% corresponding to a delivery of 1.76 mg of LCB1) indicating the low tendency of the powder to stick on the inhaler swirling chamber and mouthpiece. The HPMC capsules employed, designed for DPI, also limited adhesion of the powder to the internal wall. The distribution of the powder in the impactor was characterized by a low amount (15%) in the induction port with more substantial fractions (up to 20%) depositing on stages 2 and 3 (Fig. 5). Surprisingly, a relatively high mass of powder (24%) was collected from stage 5 to MOC where only particles with aerodynamic diameter < 1.6 μm can deposit. This favorable aerodynamic distribution produced an FPD of 1.03 mg, corresponding to a FPF of 58.6% and an MMAD of 3.09 μm. The LCB1-DPI also displayed a high extra-fine dose (0.55 mg) that should promote peripheral pulmonary deposition. It has been widely reported (Alipoor et al., 2020) that SARS-CoV-2 can spread into the deep lung area and then translocate into the bloodstream. Deposition of the LCB1 decoy in the peripheral region of the lungs could thus make virus neutralization even more effective, avoiding the onset of pneumonia and ARDS. Peripheral lung deposition may also restrain the virus from spreading to other organs where ACE2 is expressed (*e.g.*, heart, kidney, liver, and CNS), thus contributing to the prevention of multiorgan failure.

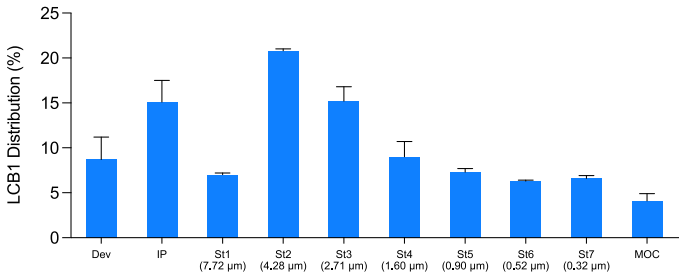

Fig. 5. Aerodynamic distribution of the LCB1-DPI in the NGI expressed as percentage of LCB1 found in the device (Dev), Induction Port (IP), stages (St) 1 to 7 and Micro Orifice Collector (MOC), (n=3, mean ± std. dev.) In the brackets the effective cut-off diameter of stages.

The high respirability of LCB1-DPI is the result of the positive characteristics of the formulation described in this work, as well as a higher delivery efficiency of the RS01 device compared to others tested (data not shown). The RS01 device employs a spinning capsule mechanism driven by centrifugal force, which is capable of de-aggregating the powder due to its prolonged exposure to turbulent air flows and the high number of particles impacts with the device walls (Buttini et al., 2021). Moreover, the powder formulation is composed of low-density

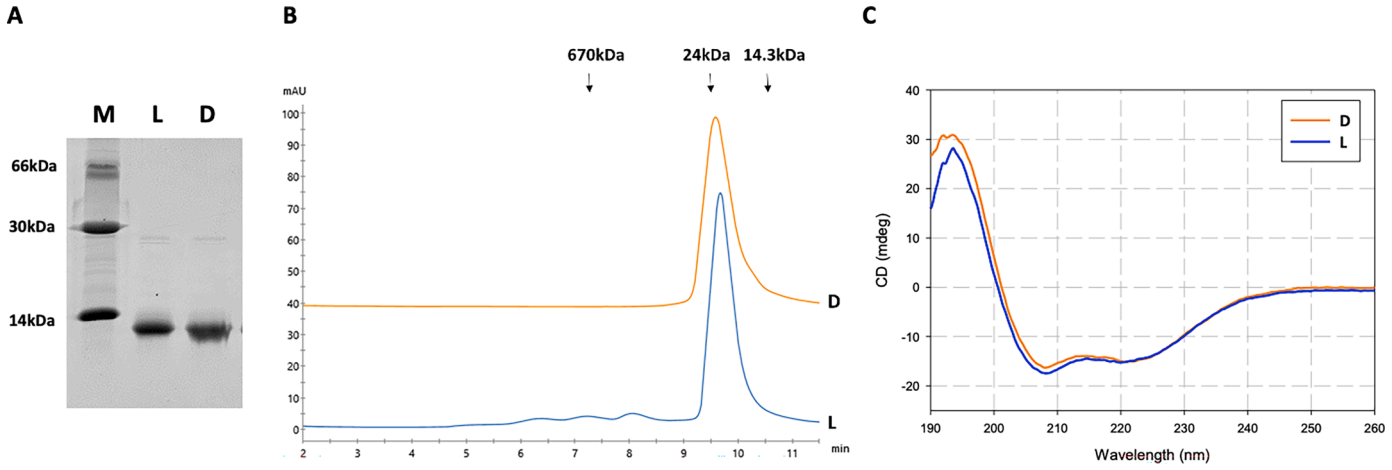

Fig. 4. SDS-PAGE (A), SEC analysis (B) and comparative circular dichroism (C) of the liquid form LCB1 control (L) and of the solubilized LCB1-DPI (D). Lanes in SDS-PAGE correspond to molecular mass markers (M) and to the samples tested. The chromatograms in panel (B) were obtained on a Superose 6 Increase 5/150 GL column detected at 280 nm. The elution positions and sizes of the molecular mass standards (thyroglobulin, trvpsinogen, lysozyme, from left to right) are indicated by black arrows.

Table 4
Aerodynamic parameters of the spray-dried LCB1-DPI aerosolized with RS01 device. The powder mass loaded in each capsule was 40 mg containing 2.16 mg of LCB1 protein (n=3, mean ± std. dev.).

	Recovered dose (mg)	Emitted dose (mg)	MMAD (μm)	FPD <5 μm (mg)	FPF <5 μm (%)	EFPD <2 μm (mg)	EFPF <2 μm (%)
LCB1-DPI	1.96±0.16	1.76±0.09	3.09±0.02	1.03±0.30	58.6±1.9	0.55±0.12	31.3±1.5

microparticles resulting from their empty internal cavity and unique crumpled-paper shape that was evidenced by SEM imaging (Fig. 3B), which should be less likely to phagocytosed by alveolar macrophages and thus exhibit a longer tissue half-life than to non-porous particles (Gharse and Fiegel, 2018).

Furthermore, the fact that the protein also exhibits good stability in solution (up to 24 h at room temperature) could lead us to hypothesize it has potential for administration by nebulization, despite the known disadvantages of these delivery systems. However, when 2.4 mg doses of decoy product were delivered from a range of nebulizers, the results were highly variable depending on the specific device used (see Table S1 in supplementary materials). The highest ED obtained was 0.82 mg, significantly lower than the result with the LCB1-DPI (1.76 mg). The poor delivery efficiency led in all cases to low FPD values (0.3-0.5 mg), more than halved compared to the powder. Also, the value of MMAD > 3.9 μm, obtained from all nebulizers, would not favor peripheral deposition of the product. The poor results for all these systems are in part due to a significant amount of the loaded product being retained in the device at the end of the administration and because part of the generated aerosol escapes into the environment (Lavorini et al., 2019; Rossi et al., 2018). Finally, an important additional aspect that should be checked is the protein integrity after the stress imparted by the nebulizer. In fact, it was recently demonstrated that the activity of alpha-1 antitrypsin decreased to 60 or 70% after aerosolization with a jet or mesh nebulizer (Bianchera et al., 2023).

In summary, the data demonstrate a clear superiority of the respirability of the protein when delivered from a DPI device compared with a liquid for nebulization.

Another important problem of spray-dried biologics is their long-term physicochemical stability especially in non-refrigerated conditions. The particles must not aggregate to form powders that cannot be redispersed, and the protein must maintain its structure unaltered even without cold chain storage. To address this point, the aerodynamic and protein stability parameters were analyzed for an LCB1-DPI stored for 12 months at 25 °C and 60% RH. The emitted dose was maintained at 85% and the RF, determined gravimetrically in the FSI, was 55%, both very similar to the corresponding values measured on the powder just after its production. The protein content of the stored powder, estimated by semi-quantitative SDS-PAGE analysis, was 6.2%, which is very close to the 5.7% content value measured at time zero. The SEC profile of the stored LCB1-DPI was also undistinguishable from that of LCB1 in solution, used as control (Fig. S1 in Supplementary materials). Altogether, these data strongly demonstrate the physicochemical stability of the LCB1 powder and its protein component over the investigation period. This result may be due to the combined effect of the two excipients used for the spray dried formulation, *i.e.,* a sugar and an amino acid, which are reported to increase the storage stability of protein-based formulations. Trehalose has in fact been reported to be superior at stabilizing proteins to other sugars because of its greater ability to form H-bonded networks with proteins, thus preventing their physicochemical degradation (Pinto et al., 2021). In addition, L-leucine is reported to displace proteins from adsorption sites at the air-liquid interface, thus reducing aggregation (Eedara et al., 2021).

3.4. Functional integrity and virus neutralization capacity of the LCB1-DPI

The functional integrity of spray-dried LCB1 was assessed by ELISA, which, as shown in Fig. 6, did not reveal any significant statistical difference in RBD binding capacity between the LCB1-DPI and the native protein in solution (control). Although indirectly, this strongly suggests that the overall native conformation of the protein was fully preserved after spray drying.

A closer correlation to the protection potential was obtained by measuring the ability of the LCB1-DPI to block internalization of a spike (SARS-CoV-2) pseudotyped lentivirus by hACE2 expressing mammalian cells. In relation to the neutralization capacity, it is important to underline that the ACE2-RBD interaction involves amino acid residues that may differ among different SARS-CoV-2 variants (Yi et al., 2022). This, together with the reduced size of the decoys and the fact that they do not cover the entire surface of the ACE2-RBD interaction, has led to some cases of variant-restricted protection (*i.e.*, the ability of a given decoy to neutralize a certain subset of SARS-CoV-2 variants) (Huang et al., 2022; Zhang et al., 2023).

As shown in Fig. 7, neither the liquid nor the dry-powder form of LCB1 were able to hinder cell penetration by the Omicron pseudo-virus and behaved essentially as the blank-powder negative control. This negative result is in keeping with the loss of Omicron neutralization potency previously reported for the monomeric form of LCB1 and other first generation mini-binders such as AHB2 (Hunt et al., 2023), but also for a range of variant-restricted mAbs (McCallum et al., 2021). This limit could be bypassed by a relatively simple modification to the amino acid structure without impacting the protein physicochemical characteristics. In fact, site-specific as well as more drastic structural modifications of the ACE2 decoys have recently been found to be required to counteract the RBD sequence changes associated with certain variants (*e.g.*, omicron variant) and to uphold their virus binding and neutralization capacity (Hunt et al., 2023). In addition to their relative ease of adaptation to novel variants, decoys, because of their small size, can accumulate on the viral surface and reach spike regions not accessible to

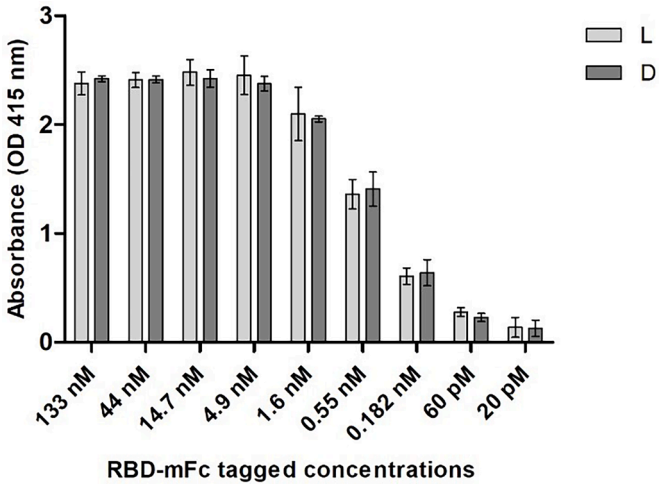

Fig. 6. ELISA assay results for the liquid form LCB1 control (L) and for the solubilized LCB1-DPI (D).

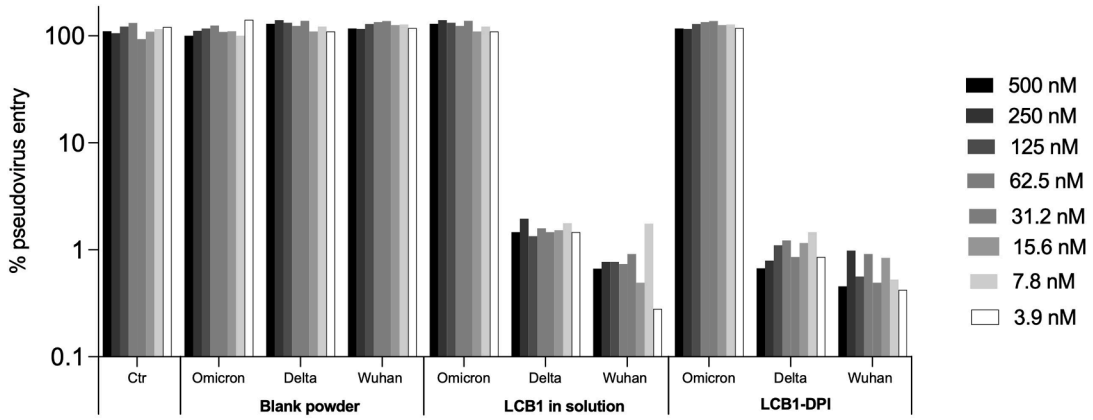

Fig. 7. Neutralization ability expressed as % pseudovirus entry with respect to the not treated wells (control, Ctr). Lentiviruses pseudotyped with the spike protein from different SARS-CoV-2 variants (Omicron, Delta e Wuhan) were tested. Pseudovirus internalization blockage data are shown for the indicated range (3.9-500 nM) of the blank powder (*i.e.* excipient only spray-dried powder), the liquid form LCB1 and the LCB1-DPI (n=3, mean values; st. dev. not appreciable as equal to zero).

much larger proteins such as mAbs (Case et al., 2021).

In contrast to the Omicron results, and in accordance with previous neutralization data (Case et al., 2021), an almost complete blockage of Wuhan and Delta pseudo-virus internalization was observed at all tested concentrations with both the liquid and the dry powder form of LCB1, pointing once again to the structural and functional integrity of the spray-dried binding protein, which maintained its integrity despite the manufacturing process.

No significant statistical differences in neutralization capability were revealed by a two-way ANOVA test applied to the two formulations investigated.

3.5. Pharmacokinetics of the LCB1-DPI

The plasma profile of native protein solution and the LCB1-DPI and the maintenance of its neutralizing capacity were investigated to confirm that the structure retained its neutralization activity even after pulmonary administration and absorption into the bloodstream.

To obtain the *in vivo* half-life of LCB1, the two LCB1 formulations were administered intratracheally to two groups of rats, blood samples, were collected at predetermined time points after treatment (up to 48 h) and were tested for LCB1 by ELISA.

As shown in Fig. 8A, in both groups, LCB1 was clearly detectable at 1 and 3 h following administration but was sharply decreased after 6 h and dropped to background levels thereafter. Importantly, very similar pharmacokinetic time-courses were observed with the liquid and the solid form of LCB1, and no statistically significant difference was revealed by a Mann Whitney test applied to the two groups. This result suggests that the formulation rapidly dissolves in the lung, and the excipients do not delay or interfere with its translocation into the plasma.

Superimposable results in terms of LCB1 persistence were obtained from Wuhan pseudovirion neutralization experiments performed on the same plasma samples utilized for ELISA (Fig. 8B). Also in this experimental set-up, LCB1 neutralization activity was maximal 1 h after administration, sharply decreased by 3 h after which it became undetectable. No statistically significant differences were detected between the two groups which supports the claim that the protein in the form of a powder had a similar fate to the liquid solution after its deposition on the lung epithelial lining fluid. The maintenance of an efficient extent of neutralization is an indication that the administered dose was able to prevent possible losses of the product due to metabolization by local peptidases, *in situ* aggregation with consequent reduction in biological activity and phagocytosis by alveolar macrophages (Chang et al., 2021).

We also examined the presence of LCB1 in BALF samples collected immediately after animal sacrifice, *i.e.*, at approximately 48 h after the initial administration of the two forms of LCB1. As expected, based on our prior data, no protein could be detected by ELISA in these late-time BALF samples, indicating a very high clearance rate of this small protein.

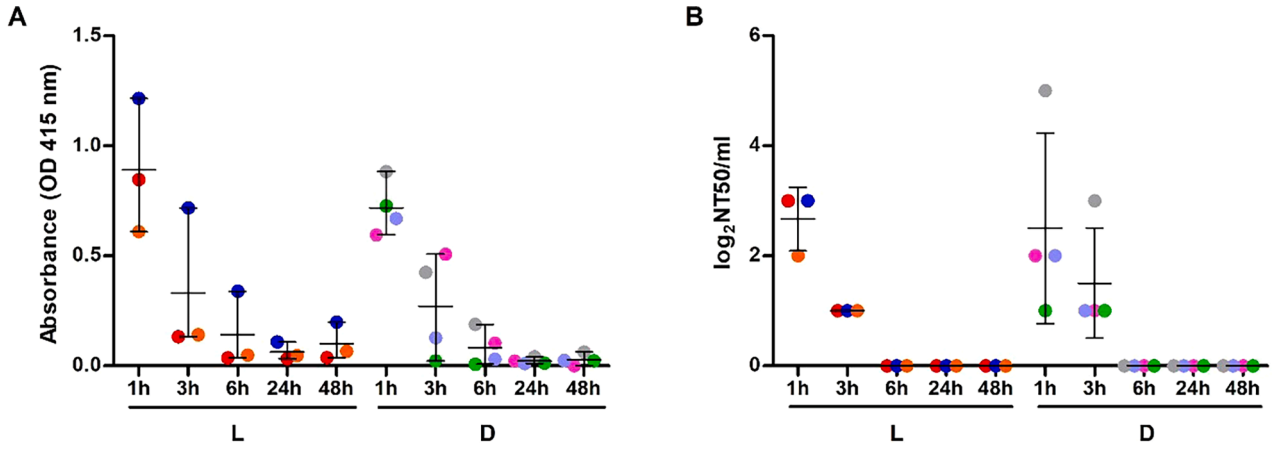

Fig. 8. ELISAs (A) and neutralization assays (B) performed on rat plasma samples collected at different times after administration of the liquid (L) or the dry-powder form (D) of LCB1. Neutralizing activity is expressed as neutralization titer 50 (NT50/mL), *i.e.*, the maximal dilution of sera from LCB1-treated rats causing a ≥50 % reduction of the signal (n=3). Individual animals, which served as biological replicates, are indicated by differently colored dots. Data were normalized with respect to corresponding control values measured in untreated animals.

It is in fact known that one of the factors affecting the residence time of a protein depends on its molecular weight: the smaller the protein is, and the shorter is the time required for it to be absorbed, assuming the absence of active transport processes (Koussoroplis and Vanbever, 2013). As an example, insulin, with a molecular weight of about half that of LCB1, has been reported being absorbed into the plasma within 15 min after pulmonary administration, indicating that its residence time in the lung is very short (Quarta et al., 2020). Considering that SARS-CoV-2 has extra-pulmonary effects as well, the rapid passage of the LCB1 into the plasma should be of undoubted benefit.

4. Conclusions

The work demonstrates how the biological activity of a protein was preserved after its presentation as an inhalation powder, by an optimized spray-drying process, and maintained after pulmonary *in vivo* administration. LCB1 was used as a small protein model able to interact with the SARS-CoV-2 spike protein, preventing the entry of virus into the respiratory host cell.

The powder exhibited high respirability both in terms of fine and extra-fine particle dose (58.6% and 31.3%, respectively) which is promising for peripheral pulmonary deposition, a feature extremely important considering that the onset of pneumonia and ARDS occurs in the alveolar region.

The decoy was rapidly translocated into the bloodstream thanks to the fast-releasing excipients included in the formulation. LCB1 protein, after its isolation from plasma, showed an effective neutralizing action against SARS-CoV-2 indicating that the biological structure had not suffered any damage during manufacture and administration. The neutralization of the circulating virus is extremely important considering that SARS-CoV-2 can affect many areas of the body where hACE2 is expressed, leading to other, non-pulmonary diseases.

Overall, this innovative delivery platform has the potential to be employed to formulate and deliver other modified decoys, both active against newly emerging SARS-CoV-2 variants or against other types of viruses. Furthermore, by tailoring the formulation strategy the platform can be easily applied to the lung delivery of therapeutic small heat-resistant proteins and peptides.

This approach represents a safe, scalable and patient-friendly method to tackle not only lung infections but many other lung disease burdening healthcare systems globally.

Funding statement

This work benefited from the equipment available within the COMP-HUB Initiative, funded by the "Departments of Excellence" program of the Italian Ministry for Education, University and Research (MIUR, 2018–2022). This work was also supported by a grant from the University of Parma, Italy (Extraordinary University Call for Biomedical Research Projects in the Field of SARS-CoV-2 and COVID-19—2020) and from the Italian Ministry of Education, University and Research (Competitive Projects MUR ex DM 1059/2021).

CRediT authorship contribution statement

Stefania Glieca: Investigation, Writing – original draft. **Davide Cavazzini:** Investigation. **Elisabetta Levati:** Investigation. **Valentina Garrapa:** Investigation, Formal analysis. **Angelo Bolchi:** Investigation. **Valentina Franceschi:** Investigation. **Simone Odau:** Formal analysis. **Simone Ottonello:** Conceptualization. **Gaetano Donofrio:** Methodology. **Jonas Füner:** Resources. **Fabio Sonvico:** Formal analysis. **Ruggero Bettini:** Conceptualization, Writing – review & editing. **Barbara Montanini:** Conceptualization, Funding acquisition. **Francesca Buttini:** Conceptualization, Supervision, Writing – review & editing.

Declaration of Competing Interest

None of the authors have any conflicts of interest or financial ties to disclose.

Data availability

Data will be made available on request.

Acknowledgments

The authors thank Qualicaps (Madrid, Spain) and Plastiape (Oggiono (LC), Italy) for providing capsule and inhalers, respectively. FB sincerely thanks Professor Christopher Marriott for his always prompt availability in proofreading the text.

Supplementary materials

Supplementary material associated with this article can be found, in the online version, at doi:10.1016/j.ejps.2023.106609.

References

Alhajj, N., O'Reilly, N.J., Cathcart, H., 2021. Leucine as an excipient in spray dried powder for inhalation. Drug Discov. Today 26, 2384–2396. https://doi.org/10.1016/j.drudis.2021.04.009.

Alipoor, S.D., Jamaati, H., Tabarsi, P., Mortaz, E., 2020. Immunopathogenesis of pneumonia in covid-19. Tanaffos 19, 79–82.

Bianchera, A., Vilardo, V., Giaccari, R., Michielon, A., Bazzoli, G., Buttini, F., Aiello, M., Chetta, A., Bruno, S., Bettini, R., 2023. Nebulizers effectiveness on pulmonary delivery of alpha-1 antitrypsin. Drug Deliv. Transl. Res. 13 (10), 2653–2663. https://doi.org/10.1007/s13346-023-01346-3.

Brun, E.H.C., Hong, Z.Y., Hsu, Y.M., Wang, C.T., Chung, D.J., Ng, S.K., Lee, Y.H., Wei, T. T., 2023. Stability and activity of interferon beta to treat idiopathic pulmonary fibrosis with different nebulizer technologies. J. Aerosol Med. Pulm. Drug Deliv. 36, 55–64. https://doi.org/10.1089/jamp.2022.0020.

Buttini, F., Quarta, E., Allegrini, C., Lavorini, F., 2021. Understanding the importance of capsules in dry powder inhalers. Pharmaceutics 13 (11), 1936. https://doi.org/10.3390/pharmaceutics13111936.

Cao, L., Goreshnik, I., Coventry, B., Case, J.B., Miller, L., Kozodoy, L., Chen, R.E., Carter, L., Walls, A.C., Park, Y.J., Strauch, E.M., Stewart, L., Diamond, M.S., Veesler, D., Baker, D., 2020. De novo design of picomolar SARS-CoV-2 miniprotein inhibitors. Science 370, 426–431. https://doi.org/10.1126/science.abd9909.

Case, J.B., Chen, R.E., Cao, L., Ying, B., Winkler, E.S., Shrihari, S., Kafai, N.M., Bailey, A. L., Xie, X., Ravichandran, R., Carter, L., Stewart, L., Baker, D., Diamond, M.S., M, T. A., Programs, I., 2021. Ultrapotent miniproteins targeting the receptor-binding domain protect against SARS-CoV-2 infection and disease in mice. Cell Host Microbe 29 (7), 1151–1161.e5. https://doi.org/10.1016/j.chom.2021.06.008.

Chang, R.Y.K., Chow, M.Y.T., Khanal, D., Chen, D., Chan, H.K., 2021. Dry powder pharmaceutical biologics for inhalation therapy. Adv. Drug Deliv. Rev. 172, 64–79. https://doi.org/10.1016/j.addr.2021.02.017.

Chen, Y., Mutukuri, T.T., Wilson, N.E., Zhou, Q., 2021. Pharmaceutical protein solids: drying technology, solid-state characterization and stability. Adv. Drug Deliv. Rev. 172, 211–233. https://doi.org/10.1016/j.addr.2021.02.016.

Costantino, H.R., Andya, J.D., Nguyen, P.A., Dasovich, N., Sweeney, T.D., Shire, S.J., Hsu, C.C., Maa, Y.F., 1998. Effect of mannitol crystallization on the stability and aerosol performance of a spray-dried pharmaceutical protein, recombinant humanized anti-IgE monoclonal antibody. J. Pharm. Sci. 87, 1406–1411. https://doi.org/10.1021/js9800679.

Donofrio, G., Franceschi, V., Macchi, F., Russo, L., Rocci, A., Marchica, V., Costa, F., Giuliani, N., Ferrari, C., Missale, G., 2021. A simplified SARS-CoV-2 pseudovirus neutralization assay. Vaccines 9(4), 389. https://doi.org/10.3390/vaccines9040389.

Eedara, B.B., Alabsi, W., Encinas-basurto, D., Polt, R., Mansour, H.M., 2021. Spray-dried inhalable powder formulations of therapeutic proteins and peptides. AAPS PharmSciTech. 22 (5), 185. https://doi.org/10.1208/s12249-021-02043-5.

Fathe, K., Ferrati, S., Moraga-Espinoza, D., Yazdi, A., Smyth, H.D.C., 2016. Inhaled biologics: from preclinical to product approval. Curr. Pharm. Des. 22, 2501–2521. https://doi.org/10.2174/1381612822666160210142910.

Gharse, S., Fiegel, J., 2018. Large porous hollow particles: lightweight champions of pulmonary drug delivery. Physiol. Behav. 176, 139–148. https://doi.org/10.2174/1381612822666160128145356.

Huang, X., Kon, E., Han, X., Zhang, X., Kong, N., Mitchell, M.J., Peer, D., Tao, W., 2022. Nanotechnology-based strategies against SARS-CoV-2 variants. Nat. Nanotechnol. 17, 1027–1037. https://doi.org/10.1038/s41565-022-01174-5.

Hunt, A.C., Case, J.B., Park, Y.J., Cao, L., Wu, K., Walls, A.C., Liu, Z., Bowen, J.E., Yeh, H. W., Saini, S., Helms, L., Zhao, Y.T., Hsiang, T.Y., Starr, T.N., Goreshnik, I., Kozodoy, L., Carter, L., Ravichandran, R., Green, L.B., Matochko, W.L., Thomson, C. A., Vögeli, B., Krüger, A., VanBlargan, L.A., Chen, R.E., Ying, B., Bailey, A.L., Kafai, N.M., Boyken, S.E., Ljubetič, A., Edman, N., Ueda, G., Chow, C.M.,

Johnson, M., Addetia, A., Navarro, M.J., Panpradist, N., Gale, M., Freedman, B.S., Bloom, J.D., Ruohola-Baker, H., Whelan, S.P.J., Stewart, L., Diamond, M.S., Veesler, D., Jewett, M.C., Baker, D., 2023. Multivalent designed proteins neutralize SARS-CoV-2 variants of concern and confer protection against infection in mice. Sci. Transl. Med. 14 (646), eabn1252. https://doi.org/10.1126/scitranslmed.abn1252.

Koussoroplis, S., Vanbever, R., 2013. Peptides and proteins: pulmonary absorption. In: Encyclopedia of Pharmaceutical Science and Technology, 4th ed., pp. 2607–2618 UK.

Lavorini, F., Buttini, F., Usmani, O.S., 2019. 100 years of drug delivery to the lungs. Handb. Exp. Pharmacol. 260, 143–159. https://doi.org/10.1007/164_2019_335.

Li, C., Ji, F., Wang, Liang, Wang, Liping, Hao, J., Dai, M., Liu, Y., Pan, X., Fu, J., Li, L., Yang, G., Yang, J., Yan, X., Gu, B., 2020. Asymptomatic and human-to-human transmission of SARS-CoV-2 in a 2-family cluster, Xuzhou, China. Emerg. Infect. Dis. J. 26, 1626. https://doi.org/10.3201/eid2607.200718.

Majumder, J., Minko, T., 2021. Recent developments on therapeutic and diagnostic approaches for COVID-19. AAPS J 23 (1), 14. https://doi.org/10.1208/s12248-020-00532-2.

McCallum, M., Walls, A.C., Sprouse, K.R., Bowen, J.E., Rosen, L.E., Dang, H.V, De Marco, A., Franko, N., Tilles, S.W., Logue, J., Miranda, M.C., Ahlrichs, M., Carter, L., Snell, G., Pizzuto, M.S., Chu, H.Y., Van Voorhis, W.C., Corti, D., Veesler, D., 2021. Molecular basis of immune evasion by the Delta and Kappa SARS-CoV-2 variants. Science 374 (1979), 1621–1626. https://doi.org/10.1126/science.abl8506.

Mutukuri, T.T., Ling, J., Du, Y., Su, Y., Zhou, Q.T., 2022. Effect of buffer salts on physical stability of lyophilized and spray-dried protein formulations containing bovine serum albumin and trehalose. Pharm. Res. 40 (6), 1355–1371. https://doi.org/10.1007/s11095-022-03318-7.

Pinto, J.T., Faulhammer, E., Dieplinger, J., Dekner, M., Makert, C., Nieder, M., Paudel, A., 2021. Progress in spray-drying of protein pharmaceuticals: literature analysis of trends in formulation and process attributes. Dry. Technol. 39, 1415–1446. https://doi.org/10.1080/07373937.2021.1903032.

Quarta, E., Chierici, V., Flammini, L., Tognolini, M., Barocelli, E., Cantoni, A.M., Dujovny, G., Ecenarro Probst, S., Sonvico, F., Colombo, G., Rossi, A., Bettini, R., Colombo, P., Buttini, F., 2020. Excipient-free pulmonary insulin dry powder: pharmacokinetic and pharmacodynamics profiles in rats. J. Control. Release 323, 412–420. https://doi.org/10.1016/j.jconrel.2020.04.015.

Rossi, I., Sonvico, F., McConville, J.T., Rossi, F., Fröhlich, E., Zellnitz, S., Rossi, A., Del Favero, E., Bettini, R., Buttini, F., 2018. Nebulized coenzyme Q(10) nanosuspensions: a versatile approach for pulmonary antioxidant therapy. Eur. J. Pharm. Sci. 113, 159–170. https://doi.org/10.1016/j.ejps.2017.10.024.

Rossi, I., Spagnoli, G., Buttini, F., Sonvico, F., Stellari, F., Cavazzini, D., Chen, Q., Müller, M., Bolchi, A., Ottonello, S., Bettini, R., 2021. A respirable HPV-L2 dry-powder vaccine with GLA as amphiphilic lubricant and immune-adjuvant. J. Control. Release 340, 209–220. https://doi.org/10.1016/j.jconrel.2021.11.002.

Su, S., Wong, G., Shi, W., Liu, J., Lai, A.C.K., Zhou, J., Liu, W., Bi, Y., Gao, G.F., 2016. Epidemiology, genetic recombination, and pathogenesis of coronaviruses. Trends Microbiol. 24, 490–502. https://doi.org/10.1016/j.tim.2016.03.003.

Vehring, R., 2008. Pharmaceutical particle engineering via spray drying. Pharm. Res. 25, 999–1022. https://doi.org/10.1007/s11095-007-9475-1.

Yi, C., Sun, X., Ling, Z., Sun, B., 2022. Jigsaw puzzle of SARS-CoV-2 RBD evolution and immune escape. Cell. Mol. Immunol. 19, 848–851. https://doi.org/10.1038/s41423-022-00884-z.

Zhang, H., Lv, P., Jiang, J., Liu, Y., Yan, R., Shu, S., Hu, B., Xiao, H., Cai, K., Yuan, S., Li, Y., 2023. Advances in developing ACE2 derivatives against SARS-CoV-2. Lancet Microbe 4, e369–e378. https://doi.org/10.1016/S2666-5247(23)00011-3.